ELSEVIER

Catalysis Today 76 (2002) 271–278

CATALYSIS TODAY

www.elsevier.com/locate/cattod

Influence of the methods of TiO_2 incorporation in monolithic catalysts for the photocatalytic destruction of chlorinated hydrocarbons in gas phase

Pedro Ávila [a], Benigno Sánchez [b,*], Ana I. Cardona [b], Moisés Rebollar [a], Roberto Candal [c]

[a] *Instituto de Catálisis y Petroleoquímica, CSIC, Campus de Cantoblanco 28049 Madrid, Spain*
[b] *Departamento de Energías Renovables del CIEMAT, Avda. Complutense 22, 28040 Madrid, Spain*
[c] *INQUIMAE, Universidad de Buenos Aires Ciudad Universitaria, Pabellón 2, 1428 Buenos Aires, Argentina*

Abstract

Three different methods of fixing titanium dioxide on a monolithic, natural magnesium silicate matrix, onto-the-wall extrusion, wash-coating and sol–gel, are compared. Photo-assisted oxidation tests with chlorinated hydrocarbons, trichloroethylene (TCE) alone and in mixtures with perchloroethylene (PCE) were carried out with the monolithic photocatalysts.

Results show that the use of extruded titania monoliths provides significant advantages for best stability of anatase, porosity and resistance to loss of active phase due to erosion. Catalysts obtained by the sol–gel method maybe a good option for this application, but the coating method must still be improved.

Keywords: Photocatalysis; Titanium dioxide catalyst; VOC; TCE; Sol–gel; Monolith

1. Introduction

During the last decade, reports of photocatalytic oxidation (PCO) in the literature have contained plentiful references to positive results in the destruction of all kinds of organic compounds. Unfortunately, the authors do not take into account the long residence times and energy consumption required, so that oxidation, even with extremely slow kinetics, is considered successful after long hours of treatment [1,2].

An important part of research in the field of photocatalysis applied to the destruction of organic contaminants has focused on the improvement of catalyst performance, developing different methods of fixing the active component (in most cases, titanium dioxide) on various types of supports [3–14].

For effective industrial application, where high volumes of gas have to be treated, gas-phase detoxification must be fast in order to operate with a contact time of seconds. The use of monolithic catalysts, solid structures with bored parallel channels, enables the pressure drop caused by the passage of the gas through the catalyst to be reduced by several orders of magnitude and improves both chemical and photon contact surfaces [15].

Studies on the gas-phase photocatalytic destruction of VOCs have shown the efficiency of such catalysts in the destruction of chlorinated compounds [16]; even with a relatively small amounts of TiO_2 on the wall of the monolith [17].

* Corresponding author. Tel.: +34-91-34-66-417; fax: +34-91-34-66-037.
E-mail address: benigno.sanchez@ciemat.es (B. Sánchez).

0920-5861/02/$ – see front matter © 2002 Elsevier Science B.V. All rights reserved.
PII: S0920-5861(02)00225-0

This has led to the need to improve the distribution of TiO_2 on the outside of the catalyst, depositing it as a coating. In this study, an attempt is made to assess the effect of the coating method on its photocatalytic behaviour in the destruction of two chlorinated compounds.

2. Experimental

In this study, titanium dioxide was incorporated onto the ceramic monoliths by three different methods. Catalyst A was prepared from a TiO_2 precursor (hydroxylated titanium dioxide gel supplied by Rhöne Poulenc, BET: 250 m^2/g), which is included in the paste before extrusion, together with natural silicates used as inorganic binders, in such a way that the TiO_2 is incorporated in the monolithic matrix. Catalyst B was prepared by wash-coating a monolithic matrix made of the mentioned natural silicates with the same TiO_2 precursor. Catalyst C, was prepared by coating the monolithic matrix with a titanium oxide obtained by the sol–gel method.

The square-cell monoliths, after drying at 383 K and treating at 773 K for 4 h in air, had a 0.31 cm pitch, wall thickness of 0.11 cm and geometric surface of 832 m^2/m^3.

The extruded titania monolith was prepared as previously described [18] using a fibrous magnesium silicate as the binder. The powder components were mixed in a Naarden vertical solids mixer. Water, containing small amounts of organic additives, was added to make it plastic and provide effective lubrication during extrusion. Wet mixing was continued until uniformity was obtained. The precursor ceramic catalyst paste was moulded into a honeycomb shape by extrusion in a single-screw Bonnot extruder and the extruded green bodies were dried and calcinated at 500 °C.

A ceramic monolith made of $MgSiO_4$ was coated by immersion in a basic aqueous suspension of hydroxilated TiO_2 gel for 20 s at a rate of 20 cm/s. The process was repeated several times and in all cases the impregnated monolith was dried at ambient temperature and calcinated at 500 °C before beginning again.

TiO_2 sol–gel was prepared by hydrolysis of titanium isopropoxide (Aldrich) in abundant water acidulated with nitric acid (Merck, PA), following by peptisation at 80 °C for 16 h [19]. This procedure yields particles of 5–10 nm diameters, aggregated in 100 nm clusters.

The first sol–gel layer was applied on a monolith previously saturated in the dispersing phase (water + HNO_3, pH 1), by dipping in the TiO_2 sol at 1 cm/s followed by immediate withdrawal at the same speed. These procedures avoid absorption of excessive sol by the dry porous monolith wall, which leads to thickness, cracking and poor adherence of TiO_2 layers.

Coating of those walls not exposed to UV light was prevented by wrapping the monoliths in a Teflon film. These “coating-free” areas help the solvent to evaporate during drying. The coated monoliths were dried overnight in an oven at 40 °C. During drying, a thin film of TiO_2 gel is formed, which further evolves into a mesoporous xerogel film.

The TiO_2 film should be stabilised by an appropriate thermal treatment that allows the particles to be sintered with the closest neighbouring particles and with the magnesium silicate substrate. Firing conditions are critical to avoid sudden evaporation of water that may crack (and peel off) the TiO_2 layer. In this study, the thermal treatment consisted of 2 h at 110 °C (ramp: 1.5 °C/min), followed by 4 h at 500 °C (ramp: 3 °C/min).

The successive layers of TiO_2 were applied by dip-coating the coated monoliths (no previous saturation in the dispersing phase), at a withdrawal speed of 1 cm/min. Drying and firing were as before at 500 °C.

Samples of monolithic catalysts before and after use in the reaction were studied with the following characterisation techniques: textural and morphological properties were analysed by nitrogen adsorption and mercury intrusion porosimetry (MIP). BET surfaces were measured by nitrogen adsorption–desorption in a Micromeritics ASAP 2000. Pore-size distribution was determined by MIP using a Thermo Quest Pascal 140/240 porosimeter. Crystallite structure phases present in the catalysts were determined by X-ray diffraction (XRD) in a Philips PW1710 powder diffractometer in the 5–75° (2θ) region using Cu Kα radiation ($\lambda = 0.15418$ nm). UV-Vis diffuse reflectance spectra were obtained in a Shimadzu model 2100 UV-Vis spectrometer. Axial strength of monoliths was determined with a Chatillon LTCM universal tensile and spring tester.

The TiO_2 content and overall composition of the monoliths was determined by inductively coupled

plasma (ICP) optical emission spectroscopy (Perkin-Elmer Optima 3300DV) of a dissolution of the ground catalysts in acid solution.

Continuous-flow mode tests lasting several hours were conducted to evaluate conversion efficiencies. The photoreactor is stainless steel and has an effective 4 cm in diameter aperture enclosed by a Pyrex window. A xenon lamp illuminates the front window and the catalyst monoliths. Contaminants passed through the catalyst monolith and then analysed by direct on-line sampling using a GC-HP 6890 with FID. At predetermined times, samples of outlet gases from manually opened switches were adsorbed through Tenax, 2,6-diphenyl-*p*-phenylene oxide, for further GC–MS identification of generated by-products.

The experimental setup, methodologies and diagrams of the monolithic photoreactor and experimental apparatus have been previously described [20,21].

3. Results and discussion

The overall appearance of the catalyst surfaces are shown in Fig. 1.

Table 1 shows the TiO_2 content and textural characteristics of the catalysts studied. It maybe seen that the TiO_2 content in Catalyst A is much greater than in Catalysts B and C. Since in Catalyst A, the TiO_2 was incorporated into the green paste together with the silicate, a significant amount of the catalyst is inside the walls of the monoliths where UV light does not reach it.

Catalyst B shows irregular distribution of TiO_2 on the ceramic substrate, while on Catalyst C the titanium oxide is incorporated homogeneously over the wall of the support. Moreover, from the analysis of titanium in Table 1, it maybe concluded that the amount of TiO_2 on Catalyst C is clearly almost twice that on Catalyst B and therefore this method seems to be better than wash-coating.

Table 1 also shows catalyst composition after exposure to reaction conditions. After reaction, TiO_2 content is lower in Catalysts B and C than in the respective fresh catalysts, which is a clear indication of loss of titanium, probably due to the erosion produced by the gas flow during the reaction time. However, in Catalyst A the composition is constant, indicating that although there was some erosion, it did not affect the surface composition.

The variation in catalyst porosity indicates that in Catalyst A, the addition of TiO_2 particles during the preparatory stages prior to extrusion increases the specific surface area due to the support and there is a slight decrease in total pore volume. This could be because of inclusion of TiO_2 particles among the supporting silicate fibres [22], which changes the porous structure of the solid, increasing the size of the macropores corresponding to the spaces among the fibre bundles.

This effect can be observed in Fig. 2, where the pore volume distribution, obtained by MIP, is shown. In this figure, it is clear that for Catalyst A the inclusion of the TiO_2 particles produces a drastic change in pore distribution on the support. Only pore volume decreases due to the original space between

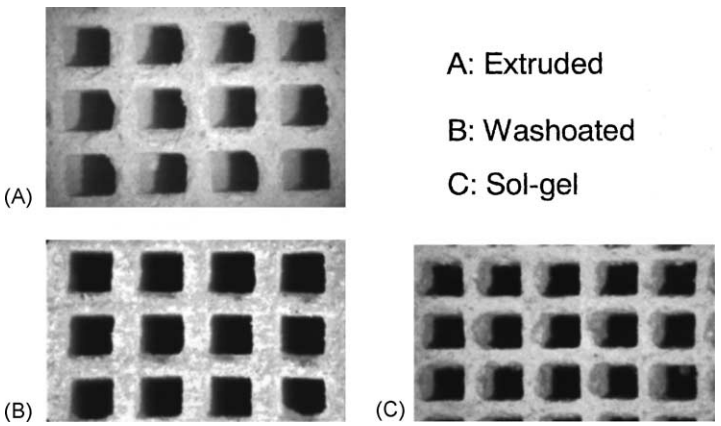

Fig. 1. Photos of the different catalysts tested.

Table 1
Characteristics of the catalyst samples used in this study

Catalysts samples	Method of preparation	TiO_2 (wt.%)	BET surface area (m^2/g)	Pore volume (cm^3/g)
Support	Extrusion	0	88	0.74
A	Extrusion	44.5	98	0.70
B	Wash-coated	2.3	84	0.62
C	Sol–gel	4.5	82	0.61
A-R	A after reaction	44.2	98	0.70
B-R	B after reaction	1.7	73	0.62
C-R	C after reaction	3.4	62	0.61

silicate fibres (40–70 nm), while the volume due to the 100 nm diameter pores, which closely corresponds to the average diameter of the TiO_2 particles, increases. Pore-size distribution in Catalyst A is bimodal with significant catalytic advantages over the original pore distribution. It is hypothesised that the increment in the specific surface area is due to the contribution of the TiO_2 particles, with a BET area of 250 m^2/g before thermal treatment.

In the case of Catalyst B (see Fig. 2), pore distribution is similar to the support alone, which is to be expected due to the small amount of TiO_2. The slight increment observed in the contribution to the total pore volume in the 20–70 nm range, maybe a consequence of the contribution of the external TiO_2 deposit, which does not modify mesopore structure. There is a general decrease in the BET area and total pore volume, which could be produced by clogging of pores having a diameter of less than 7 nm (below the MIP detection limit) by the external coating.

In the case of Catalyst C, the decrease observed in BET surface and total pore volume (Table 1) is more significant than in the cases above. Fig. 2 shows a clear decrease in the pore volume corresponding to 40–70 nm diameter pores. This maybe a consequence of clogging of those pores by TiO_2 particles. The sol–gel TiO_2 particles are much smaller than the aggregate TiO_2 precursor particles used in Catalyst B and can be generated inside the pores, plugging them. The larger amount of TiO_2 in Catalyst C compared to Catalyst B could be explained by the same phenomenon.

After exposure to reaction conditions, the textural characteristics of Catalyst A (see A-R in Table 1) remain unchanged. However in Catalysts B and C, a

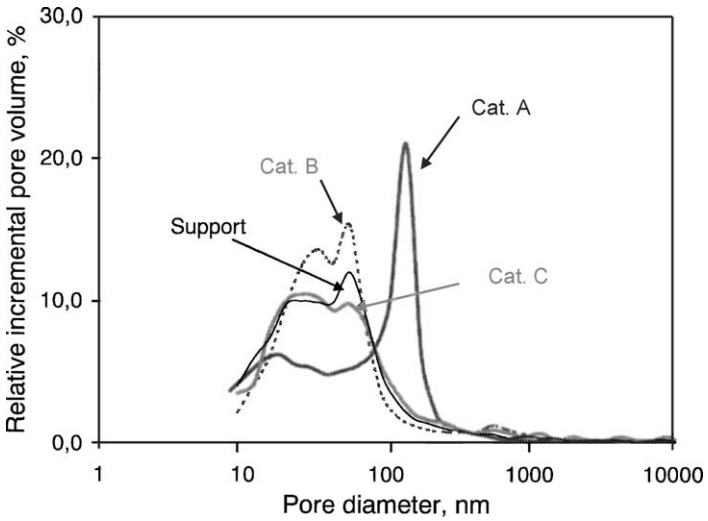

Fig. 2. Pore volume distribution of the catalysts as a function of the pore diameter.

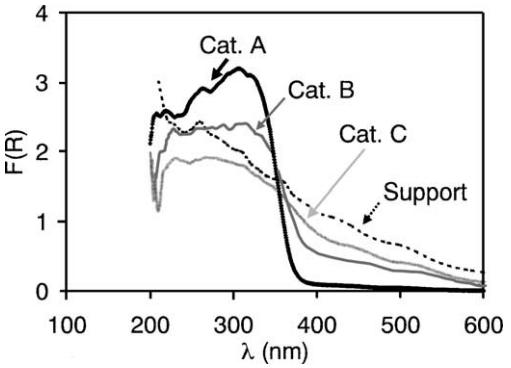

Fig. 3. UV-Vis diffuse reflectance spectra of the catalysts.

decrease in both BET surface area and total pore volume was observed (see B-R and C-R in Table 1). These results could be related to the loss of TiO_2 by erosion and with the possible deposition of carbonaceous materials during the reaction, since in the experiments carried out with the Catalysts B and C the mineralisation was not complete. Nevertheless, these results cannot be fully explained with the available data.

Fig. 3 shows the UV-Vis diffuse reflectance spectra of the catalysts. For Catalyst A, the spectrum obtained is typical of titanium dioxide, with strong absorption of radiation in the 200–380 nm range so that the band gap measured for this material was 3.3 eV (373 nm).

The spectra of Catalysts B and C are intermediate between the support and the titanium. These results are to be expected due to the low TiO_2 content in Catalysts B and C. However, the Catalyst C spectrum is more affected by the support than in Catalyst B. This behaviour maybe a consequence of the smaller particle size and low crystalinity of the sol–gel TiO_2 particles.

Fig. 4 shows XRD spectra of the catalysts and support without TiO_2. All the samples show low crystalinity. The Catalyst A XRD spectrum indicates that only the anatase phase is present in this TiO_2 sample. In the other cases, the diffractogram is mostly similar to that of the support in which the presence of magnesium silicate hydroxide (ASTM: 26-1227) and quartz (ASTM: 79-1906) are clearly identified. In Catalyst B, besides the species related to the support, rutile peaks (ASTM: 78-1510) (2θ = 27.51, 36.159, 41.3 and 54.459°) were observed. In Catalyst C, anatase was detected, and also possible traces of titanium suboxides (Ti_7O_{13}—ASTM: 18-403 and Ti_8O_{15}—ASTM: 11-473). The XRD spectra also shows peaks that could be assigned to non-stoichiometric titanium oxides phases: ASTM: 71-146 ($Ti_{1.85}O_3$) and ASTM:

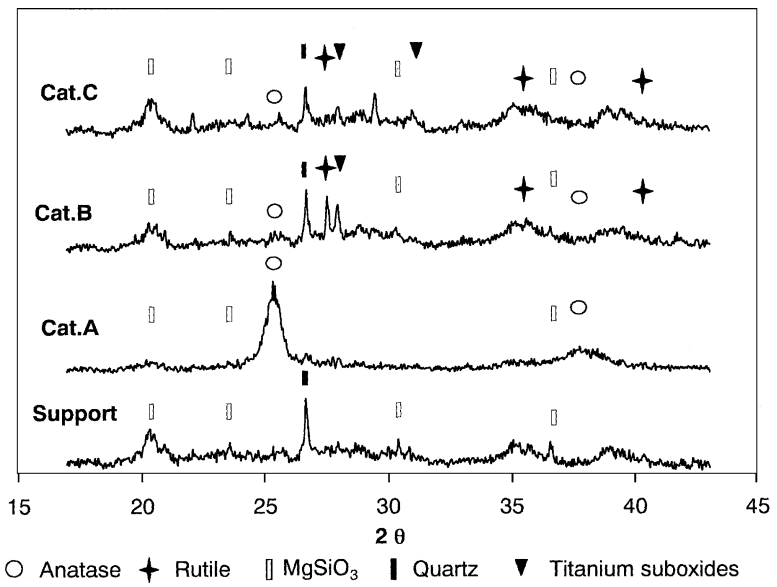

Fig. 4. XRD spectra of the catalyst.

Table 2
Reaction parameters in the photocatalytic system employed

Temperature (°C)	30–45
Concentration (ppm_v)	180
Incident photonic intensity (einstein/m^2 s)	4.23E−03
Residence time (s)	0.182–0.364
Area velocity (m/h)	4.098–8.195
Linear velocity (cm/s)	8.24–16.48
Flow rates (l/min)	0.7–1.4
Type of catalyst	Massic, impregnation, sol–gel
Irradiated area (cm^2)	102.50

18-403 (Ti_7O_{13}) that maybe produced due to incomplete oxidation of the organic precursors used during sol–gel synthesis.

Reaction parameters of the photocatalytic system are shown in Table 2. Fig. 5 shows the catalytic activity in the destruction of trichloroethylene (TCE) under the experimental conditions described in Table 2. It maybe seen that the most active catalyst is extruded A, followed by sol–gel C, with the wash-coated B the least active.

The better activity of Catalyst A could be because this catalyst contains the highest proportion of TiO_2, but this argument is not valid for Catalysts B and C, because Catalyst B is less active than C, although the proportion of TiO_2 in the wash-coated B is larger than the sol–gel-coated Catalyst C.

When the porosity of the catalysts is analysed, it maybe observed that Catalyst A has the largest surface area and pore-size. These characteristics represent a better possibility for contact between the reactants and the titanium surface, because, due to diffusion, it has more surface area and better accessibility to the pores. Catalysts B and C have very similar surface areas and pore-sizes and the differences observed in their activity cannot be attributed to these differences in porosity.

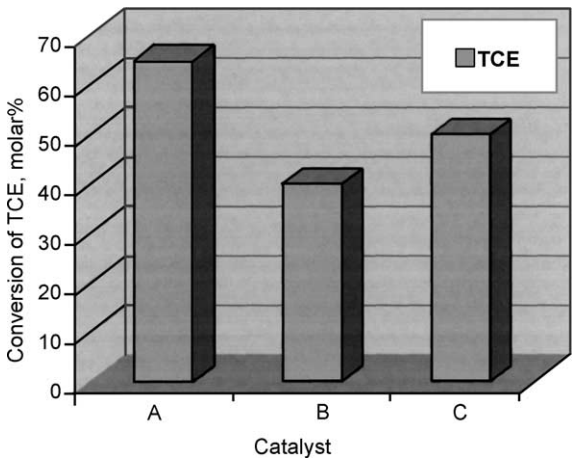

Fig. 5. Photocatalytic activity of the catalysts in TCE destruction under the operating conditions described in Table 2.

Analogously, the UV-Vis spectra reflect a better absorption capacity for Catalyst A in the range of interest (300–400 nm), that maybe related to its greater activity, but the differences observed between Catalysts B and C cannot explain the differences in their catalytic activity. The fact that Catalyst B is less active than C can be explained by the XRD results. It maybe observed in Fig. 4 that the spectrum of Catalyst B indicates that in this catalyst the TiO_2 is mainly rutile, while in Catalysts A and C the anatase phase is predominant. It is generally accepted that anatase TiO_2 is more active that rutile TiO_2 in this process [9]. Thus the loss of activity observed in Catalyst C can be assigned to this transformation and it can therefore be concluded that to prepare this type of catalyst it is necessary to avoid rutilation of the titanium dioxide during thermal treatment. It is important to notice that this transformation is not observed in Catalyst A, which is prepared with materials and heat treatment identical to B. This confirms that the inclusion of magnesium silicate in the structure of the catalyst stabilises the anatase phase, as previously demonstrated by these authors [23].

Results of the experiments carried out with mixtures of chlorinated compounds shown in Figs. 6 and 7 confirm the order of activity obtained in the tests with TCE alone. The reaction products and the stability of the monolithic catalyst are similar to those already described [21].

These figures show the results of the destruction of TCE and perchloroethylene (PCE) for the residence time of the gases in the catalytic bed. From these results, the amount of catalyst needed to achieve a given conversion value can be determined. As maybe observed for Catalyst A, destruction efficiencies are as high as 99% for residence times of 0.3 and 0.4 s for TCE and PCE, respectively.

On the other hand, Catalysts B and C required relatively longer residence times (0.4 and 0.45 s, respectively), while Catalyst B produced the worst results in the individual test as well as in mixtures.

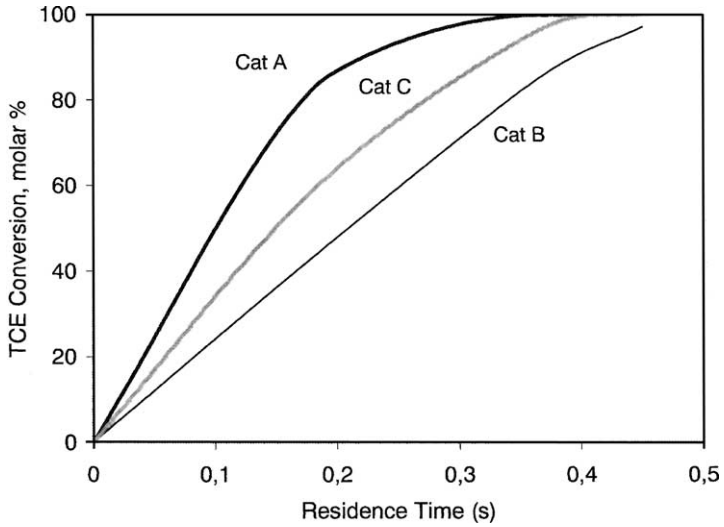

Fig. 6. TCE destruction (mixture conditions).

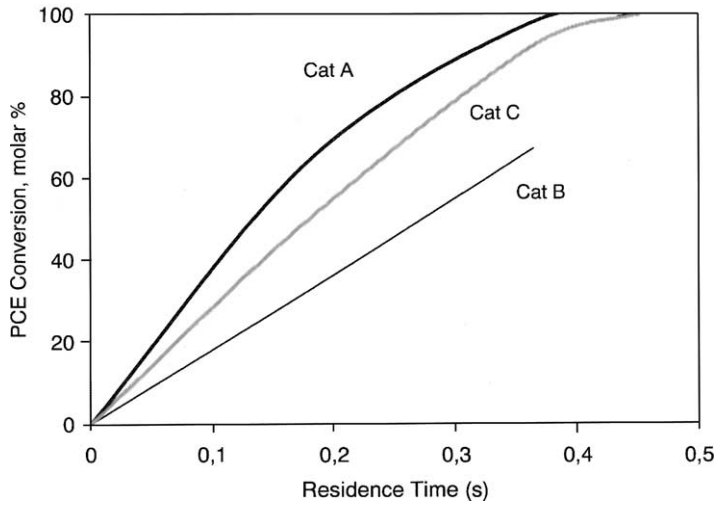

Fig. 7. PCE destruction (mixture conditions).

According to these results, Catalyst A seems to be the best catalyst for this process, but it should be recalled that the TiO_2 content in this catalyst is 10 times higher than in Catalyst C, and therefore TiO_2 activity is higher. In the evaluation of the most appropriate catalyst for this system, the price of raw materials and the manufacturing cost must also be considered.

4. Conclusions

From the results obtained in this study, it maybe concluded that Catalyst A, prepared by extrusion of a paste containing the TiO_2 precursor together with natural silicates, is the most active in the photocatalytic mineralisation of TCE and PCE, at the operating conditions in this study. Using the selected catalyst, a

residence time of 0.4 s is sufficient to obtain cleaner total destruction of TCE and PCE.

The use of the sol–gel method to obtain the TiO_2 precursor coating the monolithic support maybe considered a good option. To obtain competitive catalysts by this method, it is necessary to improve the quantity of TiO_2 added during coating and to optimise the procedure by stabilising the layers of titanium to avoid loss of material by erosion.

Acknowledgements

The authors wish to thank to the Spanish Ministry of Science and Technology (Project PPQ2001-0692-CO2-O2 and Profit FIT-140100-2001-158) and the V.C and VIII.G CYTED Networks for supporting this study.

References

[1] M.R. Nimlos, E.J. Wolfrum, D.A. Gratson, A.S. Watt, W.A. Jacoby, C.S. Turchi, NREL/TP-433-7043, Natural Renewable Energy Laboratory, USA, January 1995.
[2] Y. Parent, Sol. Energy 56 (5) (1996) 429.
[3] W.A. Zeltner, G. Hill Jr., M.A. Anderson, CHEMTECH (1993) 21.
[4] X. Fu, L.A. Clark, Q. Yang, M.A. Anderson, Environ. Sci. Technol. 30 (2) (1996) 647.
[5] H. Kominami, T. Matsuura, K. Iwai, B. Ohtani, S. Nishimoto, Y. Kera, Chem. Lett. (1995) 693.
[6] C. Anderson, A.J. Bard, J. Phys. Chem. B 101 (1997) 2611.
[7] R. Mariscal, J.M. Palacios, M. Galán-Fereres, J.L.G. Fierro, Appl. Catal. A: Gen. 116 (2) (1994) 219.
[8] A.W. Morawski, J. Grzechulska, K. Kalucki, J. Phys. Chem. Sol. 57 (6–8) (1996) 1011.
[9] G. Riegel, J.R. Bolton, J. Phys. Chem. 99 (1995) 4215.
[10] B. Pal, G. Nogami, M. Sharon, Mater. Chem. Phys. 59 (3) (1999) 254.
[11] A.D. Paola, L. Palmisano, V. Augugliaro, Catal. Today 58 (2000) 141.
[12] Z. Ding, X. Hu, P.L. Yue, G.Q. Lu, P.F. Greenfield, Catal. Today 68 (2001) 173.
[13] K.Y. Jung, S.B. Park, Appl. Catal. B: Environ. 25 (4) (2000) 249.
[14] W. Choi, J. Yun Ko, H. Park, J. Shik Chung, Appl. Catal. B: Environ. 31 (3) (2001) 209.
[15] J. Blanco, A. Bahamonde, P. Avila, B. Sánchez, M. Romero, A.J. Cardona, K.H. Funken, M. Reichert, M. Rovatti, C. Nicolella, in: EWPCA (Ed.), Acts of European Workshop on Environmental Technologies, vol. 1, Copenhagen, 1996, p. 309.
[16] B. Sánchez, M. Romero, A. Cardona, B. Fabrellas, E. García, J. Blanco, P. Avila, A. Bahamonde, J. Phys. V (France) 9 (3) (1999) 271.
[17] C. Knapp, F.J. Gil-Llambías, M. Gulppi-Cabra, P. Avila, J. Blanco, J. Mater. Chem. 7 (8) (1997) 1641.
[18] P. Avila, A. Bahamonde, J. Blanco, B. Sánchez, A. Cardona, M. Romero, Appl. Catal. B: Environ. 17 (1998) 75.
[19] B.L. Bischoff, M.A. Anderson, Chem. Mater. 7 (1995) 1772.
[20] J. Blanco, P. Avila, A. Bahamonde, B. Sánchez, M. Romero, Catal. Today 29 (1996) 437.
[21] B. Sánchez, A. Cardona, M. Romero, P. Avila, A. Bahamonde, Catal. Today 54 (1999) 369.
[22] P. Avila, J. Blanco, A. Bahamonde, C. Barthelemy, J.M. Palacios, J. Mater. Sci. 28 (15) (1993) 4113–4118.
[23] J. Blanco, P. Avila, M. Yates, A. Bahamonde, Stud. Surf. Sci. Catal. 91 (1995) 755.